Mechanics of Quantum Dots' Self-Assembly on a Periodically Poled Substrate of Lithium Niobate

Agnes Thornberg
agnes.thornberg@gmail.com

under the direction of
Assoc. Prof. Katia Gallo
Department of Applied Physics
Quantum Electronics and Quantum Optics
KTH Royal Institute of Technology

Research Academy for Young Scientists
July 13, 2016

Abstract

Recently nanoparticles known as quantum dots, consisting of solely 10-100 atoms, have been gaining recognition for their efficient energy confinement. However, it is problematic to arrange these small particles and subsequently, interest in making quantum dots self-assemble, arrange themselves into an ordered structure, has grown. In this study a substrate of lithium niobate ($LiNbO_3$) with poled domains and micro-nano structures has been used to study if the self-assembly of quantum dots is affected by the charged domains. Through the use of fluorescence imaging, the self-assembly of two types of quantum dots, positively and negatively charged, on a substrate of $LiNbO_3$ was studied. Images depicting the fluorescing quantum dots were rendered and later compared and analysed. The results indicated that the correlation between the physical morphology of the micro-nano structures and the self-assembly was stronger than the correlation between the charged domains and the self-assembly.

Contents

1 Introduction **1**

1.1 Properties and Applications of Quantum Dots 1

1.2 Lithium Niobate 6

1.2.1 Properties 6

1.2.2 Engineering Ferroelectric Domains Through the Application of an External Electric Field 7

1.3 Background to the Study 8

1.3.1 Properties of Quantum Dots with Cadmium Selenide Core 8

1.3.2 Properties of the Substrate 9

1.4 Fluorescence Imaging 10

1.5 Aim of the Study 11

2 Method **11**

3 Results **13**

3.1 Negative QD's Distribution on Patterned Sample 13

3.2 Positive QD's Distribution on Patterned Sample 16

4 Discussion **18**

4.1 Analysis of Result 18

4.2 Further Studies 20

5 Acknowledgements **20**

1 Introduction

Quantum dots (QDs), with their remarkable photo-physical properties, are rapidly gaining recognition due to their potential in both existing and emerging technologies. Potential applications include solar cells, LED screens and biological imaging. QDs are semiconductors, constituting an intermediate of conductors and insulators. Due to the nanoparticles' high fluorescent properties and their ability to emit distinct colours, they are optimal to use in imaging. However, due to their minute size, complications arise when arranging the QDs. Therefore it is of great interest to study possible methods which can cause the QDs to self-assemble, which is the process in which disordered particles form an organised structure due to local interactions. [1]

1.1 Properties and Applications of Quantum Dots

QDs are commonly referred to as artificial atoms due to their analogous physical properties with real atoms, yet differing in that QDs have tunable characteristics [1]. Like atoms, QDs are considered zero-dimensional systems, meaning that all dimensions are within the nanometre range, in contrast to for example nanowires where one dimension is outside the nanometre range or nanofilms where two dimensions are outside the nanometre range [2]. In QDs, negative electrons and their corresponding holes, or their excited states, build pairs that are confined and centralised to a single point [3], in contrast to metals whose electrons are delocalised to a common electron cloud. It is the small diameters, 2-10 nm, of the QDs that enables the beneficial ability to confine electron-hole pairs [4]. The reason for this is when crystals of semiconductors reach nanometre scale, negative electrons and positive holes experience a strong confining potential, leading to significantly discrete energy spectra within the QDs [5]. QDs consist of several atoms, which give rise to energy levels and the combination of these energy levels form bands. The ground states form what is called the valence band, and the excited states form the conduction band, that which is in between is called the bandgap or the energy gap. As

the size of the dot increases, the amount of energy levels also increase thus resulting in larger bands with more energy levels, yet smaller bandgaps [7].

Each energy level that is bound to the QD is described by a wave function. Every wave function describes the optical absorption and emission, similar to electrons bound to a nucleus in an atom [5]. A higher energy level requires higher energies of absorption, thus yielding higher energies of emission in comparison to lower energy levels. Higher energies correspond to shorter wavelengths and lower energies correspond to longer wavelengths [6]. In turn, wavelengths of different sizes correspond to different colours of light on the visible light spectrum. When an atom absorbs a photon with energy that fulfills the difference between two energy levels, the atom becomes excited. Prior to returning to ground state, and emitting a photon, fluorescing, the atom may lose some of its energy. The energy that is emitted in this case will have a longer wavelength compared to the energy that is absorbed [6], as is described in Figure 1. The same mechanism can be applied to QDs.

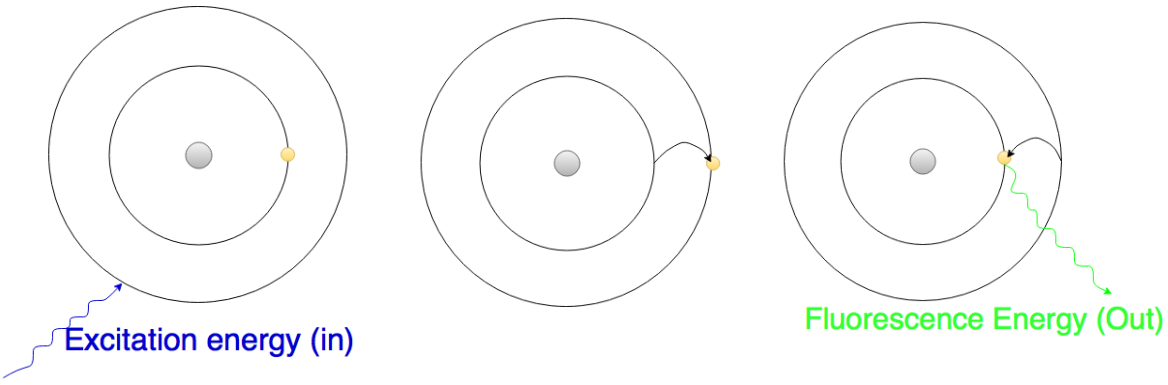

(a) Incoming energy, for example a photon, is absorbed by the atom while it is in its ground state.

(b) The absorbed energy causes the electron to enter an excited state, thus rising at least an energy level.

(c) The atom fluoresces and thereof emits energy in the form of photons, while decaying to its ground state again.

Figure 1: If an atom is provided with an energy that is equivalent to the energy difference between the excited state and the ground state the energy will be absorbed. The atom will become excited. When decaying to its ground state, energy is emitted in the form of a fluorescence photon.

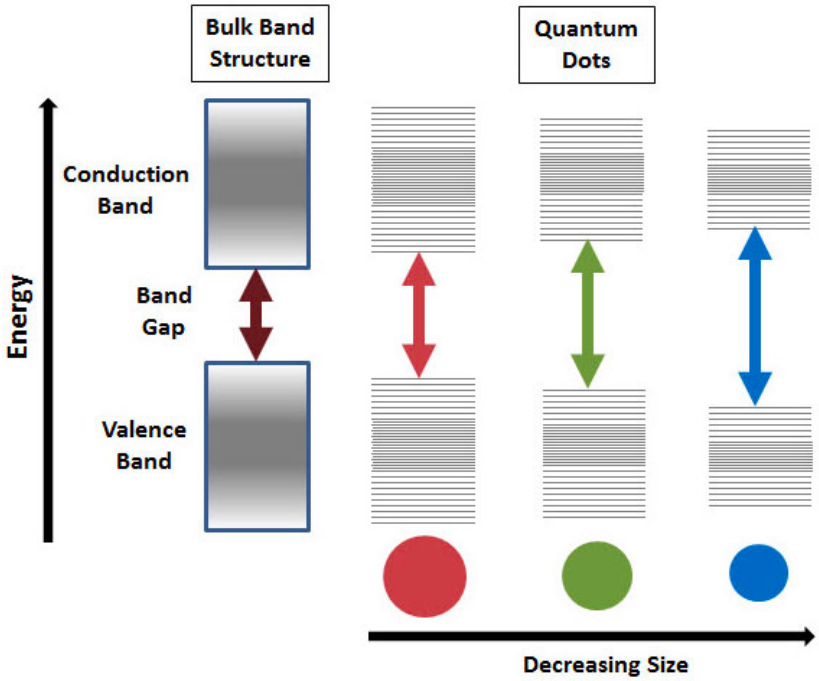

Figure 2: As the size of the dot decreases, the gap between the ground state and excited states increases. Consequently, more energy with shorter wavelengths will be emitted giving rise to different coloured fluorescence, in contrast to bulk structures that have a constant energy gap due their delocalised electrons. [1]

In QDs these optical characteristics can be adjusted simply by altering the size of the crystals [5]. Generally, as the size of the dot decreases, the difference in energy between the hole and the electron increases. When the size of the dot decreases, the amount of atoms within the particle decreases giving rise to fewer energy levels within the dot, thus the highest ground state will be further away from the lowest excited state. Consequently, more energy is required to excite the dot, which results in that more energy is emitted when it returns to the ground state, as is illustrated in Figure 2. It is therefore possible to manufacture QDs of the same material, that emit different colours of light simply by altering the size of the crystal [7].

The combination of the QD's tunable emission properties and the possibility to suspend them in an organic polymer solution, presents cheap and efficient applications in emerging and existing technologies if they manage to self-assemble. The colloidal QDs,

[1] Aldrich Materials Science. *Quantum Dots* [Online]. Sigma-Aldrich; 2016 [cited date: 2016 July 9] Available from: `http://www.sigmaaldrich.com/materials-science/nanomaterials/quantum-dots.html#applications`

QDs that are dispersed in a solution, can simply be poured onto a substrate, giving rise to low-cost fabrication. With their efficient light emission, QDs exhibit great potential to serve as a cheaper and better alternative in LED lighting and imaging, biological imaging as well as in solar cells. [8]

As aforementioned, QDs are referred to as artificial atoms. The ability to arrange the QDs into more than zero dimensions would therefore enable the manufacturing of solids with tunable properties, causing the characteristics to be dependent on the QD's properties but also the physical properties of the structures that they form. Ordered structures of nanoparticles, instead of random mixtures, provide more uniformity as well as control over the distances between the particles. Due to the small sizes of QDs, traditional methods of organising particles into structures are not possible. Subsequently, it is necessary to explore mechanisms which can cause the QDs to self-assemble. [9]

The ability to position QDs into a desired pattern would benefit all aforementioned possible areas of application. Different methods for the self-assembly of colloidal QDs that have been investigated include: electrostatics (movement of electric charges), lithography (sample patterning), dip-coating, physical confinement in moulded structures, sedimentation, capillary forces and electrophoretics (use of electric fields to manipulate movement of particles). Hammond [10] carried out a study where she investigated the possibility of using secondary interactions, such as charged interactions, hydrogen bonding, hydrophobic interactions and biological interactions, as chemical templates. This concept is called surface sorting and proved to be very efficient in means of causing the QDs to self-assemble. [10]

Another approach for assembling nanoparticles into large-scale structures was taken by Yang et. al., who analysed the possibility of using plasma lithography. Essentially, plasma lithography is patterning a substrate by treating various parts with plasma. In their study, they found that the pH of the solution that the QDs were dispersed in strongly impacted the self-assembly. Their results indicated that at low pH the QDs would favourably adhere to treated hydrophilic areas, while at high pH the QDs were

drawn to untreated hydrophobic areas, hence proving that the properties of the solution affects the self-assembly of colloidal QDs. [11]

The volatility of the solvent can greatly impact the distribution of the QDs. As the solvent evaporates, the interparticle attractions become more significant. Essentially, increasing the van der Waals attractions causes the interparticle distances to decrease, resulting in cracks of the layers that the QDs form. This negatively affects the performance of the self-assembled device. [9]

Nanoparticle rings and dendrites are other resulting patterns of solvent evaporation. Ring-like nanoparticle patterns can be explained by the Marangoni Effect. During the evaporation of volatile, quickly evaporating, solvents, significant temperature variations may occur between the solution and the free upper surface. As a result of the temperature gradient, the fluid will rise in the centre and sink down by the walls, resulting in the particle concentration being higher along the edges. Self-assembled dendrite-like structures are formed through the interplay between the solvent's mechanisms and the interactions of the particles. After complete solvent evaporation, the combination of the ordering effect of crystallisation, the disordering effects of the fluctuating nanoparticles and the drying edges will give rise to nanoparticles arranged in dendrites, as in Figure 3. [9]

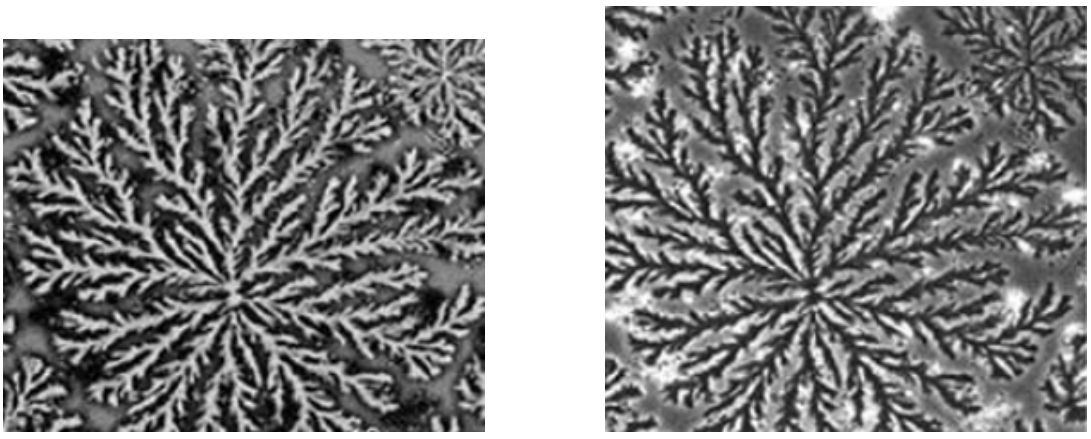

(a) Fluorescent image (b) Image depicting physical arrangement

Figure 3: Images of dendrites formed by water-solubilized CdSe/ZnS QDs upon drying and self-assembly at room temperature at 0.3 $\mathrm{mg\,ml^{-1}}$. [2]

1.2 Lithium Niobate

1.2.1 Properties

Lithium Niobate ($LiNbO_3$) is a man-made dielectric material, meaning that no free carriers of charge are available for conduction [12]. In 1949 $LiNbO_3$ was discovered to be ferroelectric [17], a dielectric material that spontaneously switches polarisation. Dielectrics belong to a group of materials, which can be polarised through the application of an external electric field. When an external electric field is applied, a polarisation is induced where the complexes of different charges within the crystal become separated. This results in dipoles within the structure. Some dielectric materials, such as $LiNbO_3$, are form polar crystalline structures, hence the complex already consists of electric dipoles. Even though the dielectric material consists of polar atoms, the applied electric field will determine the reorganisation of the charges [12].

Dielectrics that naturally contain dipoles, such as $LiNbO_3$ constitute a subgroup to dielectrics called pyroelectrics. Pyroelectrics exhibit a spontaneous polarisation without the need for application of an external electric field. Ferroelectrics are a subgroup to pyroelectrics and include materials where the spontaneous polarisation can be reoriented through the application of an electric field, which is called poling. $LiNbO_3$ exhibits two directions of possible spontaneous polarisation: up and down. When the polarisation is directed upwards it will result in a positively charged surface on the top of the structure and a negatively charged surface on the bottom of the structure, and vice versa. Ferroelectrics exhibit a distinct phase transition from a high-temperature paraelectric phase to a low-temperature ferroelectric phase. In the paraelectric phase there is no spontaneous polarisation, $(P) = 0$, while in the ferroelectric phase spontaneous polarisation may occur, which is illustrated in Figure 4. [12]

[2]V. Shevchenko E. V. Talapin D. *Self-assembly of semiconductor nanocrystals into ordered superstructures.* Argonne, IL, USA. Chicago, IL, USA: Springer Vienna; 2008: 119-169.

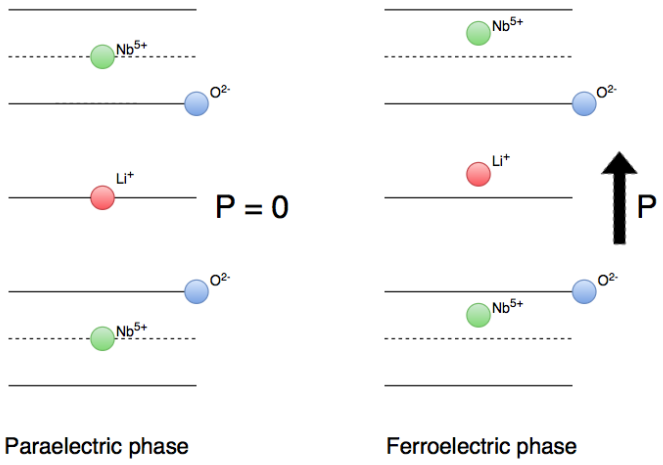

Figure 4: In the paraelectric phase there is no spontaneous polarisation, resulting in a neutral surface within the structure. In the ferroelectric phase spontaneous polarisation occurs, resulting in positively and negatively charged surfaces on top of the structure

1.2.2 Engineering Ferroelectric Domains Through the Application of an External Electric Field

Due to the ferroelectric properties of $LiNbO_3$, it is possible to manufacture domains where the polarisation is switched, resulting in areas of different charges on the substrate's surface. Initially a periodic mask of insulating photoresist is fabricated on the crystal's surface through the use of standard photolithography, as is illustrated in Figure 5a. The surface is spin-coated with photoresist, a light-sensitive material, in order to obtain an even thin film of resist. A mask consisting of chromium with desired pattern is then applied. The surface is exposed to ultra-violet light, the photoresist is developed and the irradiated areas are washed away. [16]

Following this, a conductive gel is applied in order to obtain contact between the sample and the high voltage amplifier, as is illustrated in Figure 5b. Due to the mask of photoresist, only the areas that are left uncovered will be affected by the applied electric field and switch polarisation. The remaining photoresist is washed away, which results in a substrate consisting of periodically poled domains, as seen in Figure 5c. [12]

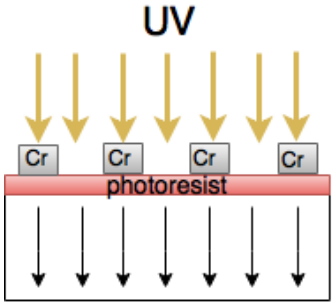

(a) Photolithography is performed to obtain a periodic pattern of photoresist

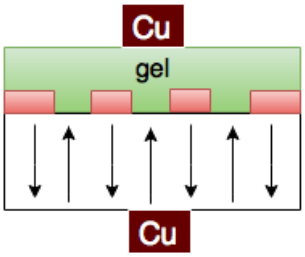

(b) Conductive gel and an external electric field is applied to sample in order to switch polarisation

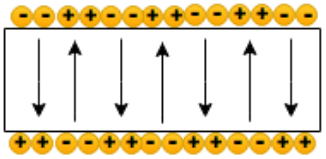

(c) Polarisation is switched in exposed areas, resulting in a surface consisting of periodically poled domains

Figure 5

1.3 Background to the Study

1.3.1 Properties of Quantum Dots with Cadmium Selenide Core

In this study QDs approx. 5-6 nm in diameter with a cadmium selenide (CdSe) core and cadmium sulphide (CdS)/zinc sulphide (ZnS) multi-shells will be examined. Two different samples of QDs will be studied, the first sample containing positively charged QDs dispersed in water and the other containing negatively charged QDs dispersed in isopropanol.

Among all QDs of the core-shell type, CdSe/ZnS are the most commonly studied. The core consisting of CdSe has the ability to cover most of the visible light spectrum, simply by adjusting its size [13]. Because of its wide bandgap, the ZnS shell has a significant ability to confine electron-hole pairs [13]. Coating QDs with a shell consisting of materials with wide bandgaps is advantageous for stabilising the fluorescence, as the shell acts like an insulator for the carriers of charge [14]. However, due to mismatch in lattices of CdSe and ZnS, QDs of this type suffer from defects [13]. Subsequently, CdS shells were introduced as an intermediate shell, forming a core-shell-shell structure [13]. By introducing additional shells, the insulation of the carriers become stronger, thus further stabilising the fluorescence and consequently giving brighter images [13]. QDs of this

type are used in cell imaging and have been proven to be less toxic than the QDs solely consisting of CdSe and ZnS [15]. Furthermore, CdSe/CdS/ZnS QDs have also been used as optical contrast agents in human pancreatic cancer cells [15].

1.3.2 Properties of the Substrate

The substrate that was used was manufactured by Mohammed Amin Baghban, at KTH Royal Institute of Technology. The sample was poled using a hexagonal-patterned mask, as is illustrated in Figure 6, with openings of 10, 30, 50, 100, 200 and 300 µm. The original polarisation was downwards, thus the surface of the top of the sample was negatively charged. In this study the 200 µm domain will specifically be studied, optical images of the domains are found in Figure 7. When the domains were fabricated, the sample was by accident turned the wrong way, resulting in that they were not made according to the sample's intrinsic structure. This resulted in that unusual micro-nano structures in the form of self-assembled dots were observed, which can be seen in Figure 8. When the polarisation of the surface was analysed using piezoresponse force microscopy (PFM), it was found that the domains had switched polarisation, but the micro-nano structures had not, as is illustrated in Figure 9.

Due to the considerably large size of the poled domains, it is expected that the polarisation is prevalent on the back of the sample as well. On top of the sample, the polarisation is directed upwards, resulting in that the surface of the domains are positively charged. The domains on the back of the sample are therefore expected to have a downwards polarisation, resulting in negative charges on the domain surfaces. It is therefore also interesting to study how the back of the sample affects the self-assembly of the QDs. The difference between the domains on top of the sample and on the back, is that the domains on the top have been edged, meaning that they have a physical morphology. It is also interesting to study if this physical morphology will affect the self-assembly. The back of the sample is illustrated in Figure 10.

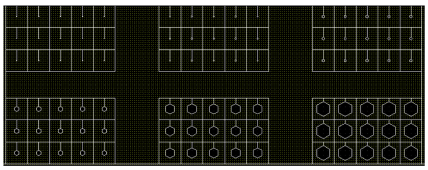

Figure 6: A polymer mask with hexagonal patterns used while poling the sample.

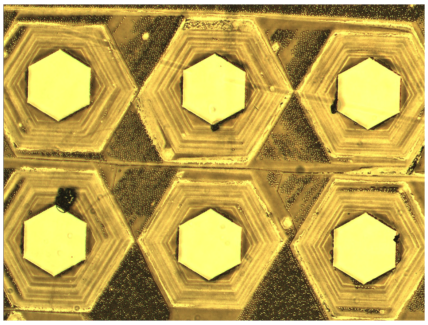

Figure 7: Image of the top of the 200 µm domains.

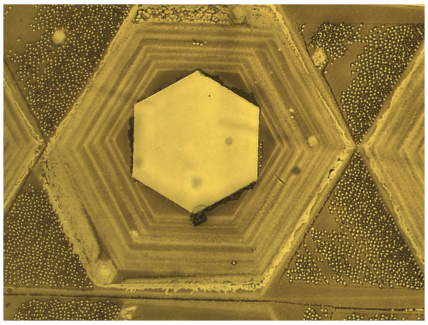

Figure 8: Image of 200 µm domain where micro-nano structures are depicted in the form of dots.

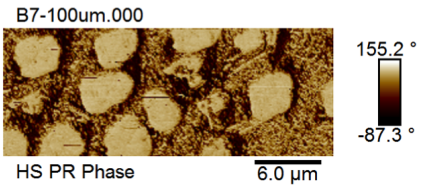

Figure 9: PFM picture of micro-nano structeres, the dark areas illustrate a change in polarisation while the light areas represent areas where no change in polarisation has occurred.

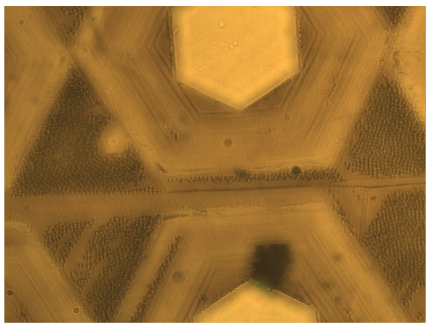

Figure 10: Image of the back of the 200 µm domain. The image of the physically edged domain's pattern that is on top of the sample penetrates through the back.

1.4 Fluorescence Imaging

Due to the fluorescent properties of QDs, fluorescence imaging is an effective technique to study the distribution of nanoparticles. A fluorescence microscope essentially functions in the same way as a traditional light microscope. The difference is that a fluorescence microscope uses a higher light intensity. The intense light excites the fluorescent species

of the sample. The species then fluoresces and emits energy with longer wavelengths than the original source. The emitted energy produces the image, which is observed by a camera. Through the use of different filters it is possible to isolate fluorescence of specific wavelengths, this will allow visualisation of only that which is fluorescing. [18]

There are four different filter blocks, which can be used to select which fluorescence to detect. Position #1, labelled B-2A, is used for species that absorb blue excitation light and emit green fluorescence. Position #2, labelled Tx Red, excites with green light for species that emit fluorescence in red light. Position #3, labelled DIA-ILL, is for all reflected light, which allows detection and imaging of all structures of a sample. Position #4 is labelled UV-2A and has an ultraviolet excitation for species that fluoresce in the blue light. [19]

1.5 Aim of the Study

The aim of this study is to analyse and understand the mechanisms of poled domains of $LiNbO_3$ that affect the self-assembling of QDs. As the structure consists of both electric and physical inconsistencies, both of these parameters will be analysed.

2 Method

The method of this study is summarised in Figure 11.

In this study two types of colloidal QDs were studied, negatively charged QDs that were dispersed in isopropanol and positively charged QDs that were dispersed in water. The fluorescence properties of the QDs were characterised through the use of a fluorescence microscope. It was not necessary to obtain exact values of excitation and fluorescence energies due to that this information only was needed to understand which filter was best suited for viewing the QDs. The differently charged QDs were studied separately. Prior to pipetting the samples, the solutions were shaken in order to avoid sedimentation or clustering. 1 µL of each QD solution was pipetted separately and placed on a non-

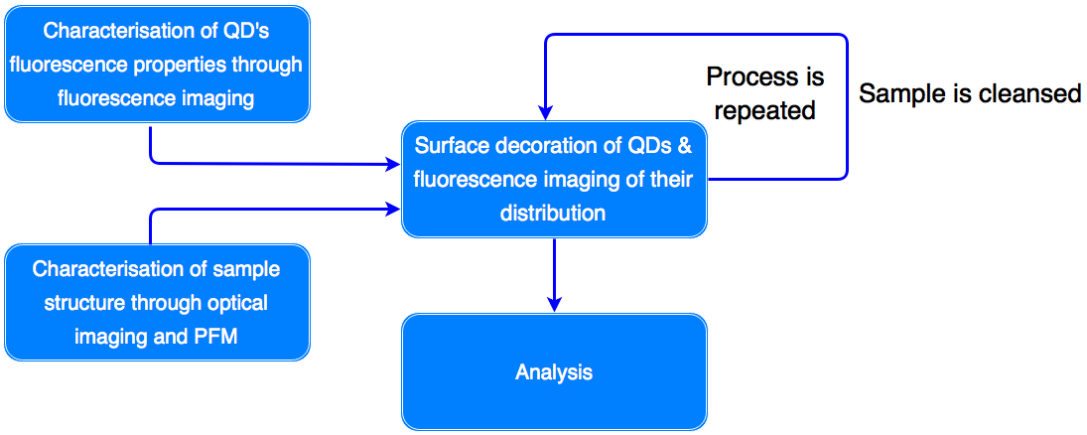

Figure 11: Flowchart depicting the method of the study.

poled sample of $LiNbO_3$, ensuring that only the QDs were studied. First the positively charged QDs were studied. Prior to studying the QDs, the droplet evaporated. After this the sample of $LiNbO_3$ with positively charged QDs was studied under the fluorescence microscope. The sample was studied using the three different fluorescing filters, B-2A, Tx Red, and UV-2AT. Digital settings were adjusted in order to obtain a clear image, the filter which gave the brightest image of the QDs was concluded to be best for the QDs fluorescence properties. The filter was recorded and used later while looking at the QDs on the patterned sample. The non-poled sample was cleaned using an ultrasonic cleaner for 5 minutes and the same procedure was repeated for the negatively charged domains.

The sample structure was characterised prior to starting this experiment through the use of standard optical imaging. The sample was placed under a light microscope, optical images at magnification 10x/0.25 were taken both of the top of the sample as well as the back of the sample. PFM, piezoresponse force microscopy, images were also taken of the micro-nanostructures in order to understand the polarisation within the structures.

Prior to applying the QDs to the patterned sample, the solution of QDs was shaken in order to avoid sedimentation or clustering. One drop containing 1 µL QDs was pipetted and applied to the top of the patterned sample. Before looking at the sample under the microscope, the droplet evaporated. The sample was observed at magnitudes 2.5x/0.075 and 100x/0.95. While the sample was observed at the different magnitudes, the filters

were adjusted. The fluorescing filters were used to view the QDs distribution and the DIA-ILL to observe the optical surface of the same areas. Digital settings were adjusted in order to obtain optimal image quality. Images were taken by a CCD camera at all magnitudes and all filters.

The sample was then cleaned by using an ultrasonic cleaner for 5 minutes, and later rinsed with water. The entire process was repeated for the back and for both types of QDs. The images that were taken with the different parameters were then analysed by studying the relationship between the fluorescence and the domain structures of different magnitudes, filters and charges.

3 Results

3.1 Negative QD's Distribution on Patterned Sample

Top of Sample

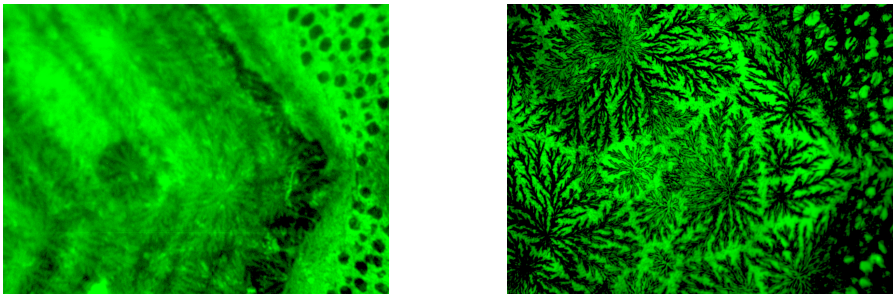

(a) B-2A filter depicting QD's fluorescence

(b) DIA-ILL filter depicting surface topology

Figure 12: Image of outer area of domain, depicting micro-nano structures. Magnification: 100x/0.95

Figure 12 depicts the negatively charged QDs arranging themselves according to dendrite-like structures due to evaporation and inter-particle interactions. However, avoiding the edged micro-nano structures, possibly because of the physical morphology or the charges of the structures.

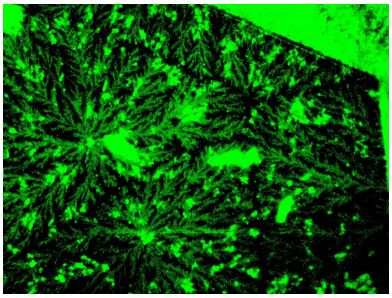

(a) B-2A filter depicting QD's fluorescence

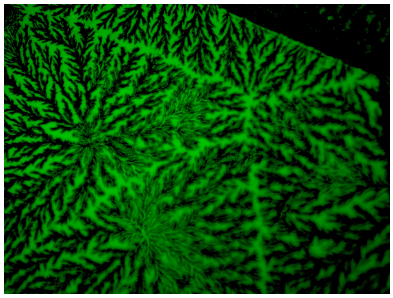

(b) DIA-ILL filter depicting surface topology

Figure 13: Image of inside of domain. Magnification: 100x/0.95

Figure 13 shows the self-assembly of the negatively charged QDs inside the positively charged domains. It is observed that the arrangement does not seem to follow the structure of the domain. However, dendrite-like structures are also present here. Seemingly, electric mechanisms are not in play.

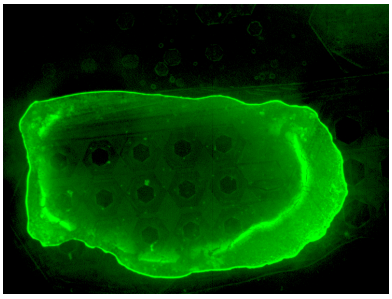

(a) B-2A filter depicting QD's fluorescence

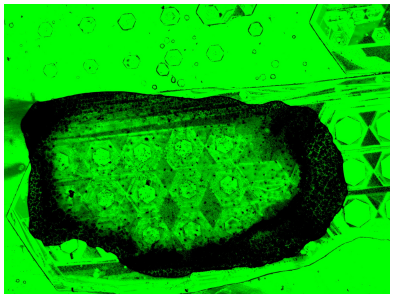

(b) DIA-ILL filter depicting surface topology

Figure 14: Image depicting the droplet after evaporation. Magnification: 2.5x/0.075

Figure 14 depicts the entire droplet of negative QDs, it is clear that the QDs have arranged themselves around the edge of the droplet, indicating that the evaporation of the solvent affects the self-assembly.

Back of Sample

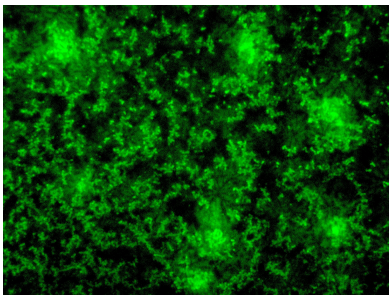

(a) B-2A filter depicting QD's fluorescence

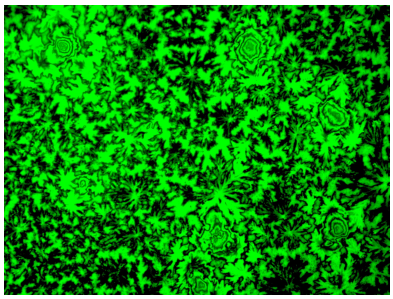

(b) DIA-ILL filter depicting surface topology

Figure 15: Image of QDs on back of domain. Magnification: 100x/0.95

Figure 15 depicts the negatively charged QDs on the back of the sample, dendrite-like structures are present yet shorter in comparison to those on the top of the sample. This may perhaps be due to the lack of physical edging or differently charged surface.

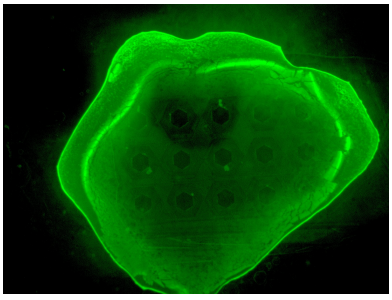

(a) B-2A filter depicting QD's fluorescence

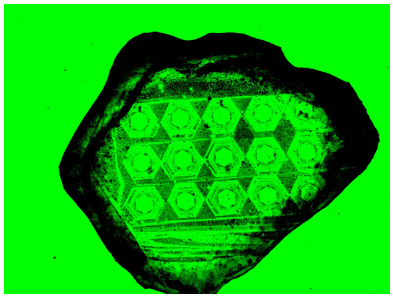

(b) DIA-ILL filter depicting surface topology

Figure 16: Image depicting the droplet after evaporation. Magnification: 2.5x/0.075

Figure 16 depicts the droplet of negatively charged QDs on the back of the sample. Just as in the image of the droplet on the top of the sample, the image of the evaporated droplet on the back of the sample depicts a higher concentration of QDs along the edges. Confirming that the evaporation affects the self-assembly of the QDs.

3.2 Positive QD's Distribution on Patterned Sample

Top of Sample

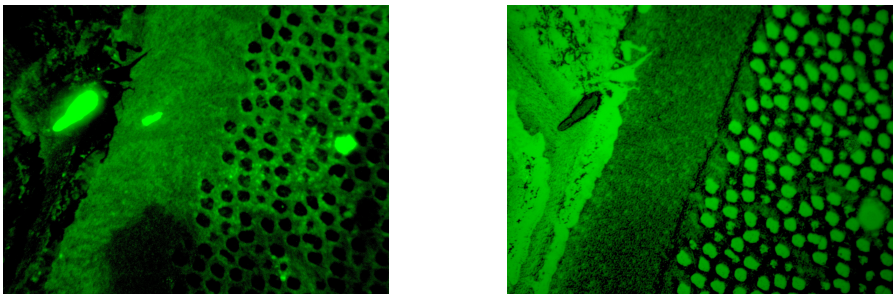

(a) B-2A filter depicting QD's fluorescence

(b) DIA-ILL filter depicting surface topology

Figure 17: Image of outer area of domain, depicting micro-nano structures. Magnification 100x/0.95.

Figure 17 illustrates positively charged QDs on the top of the sample. Just like the negatively charged QDs, the positively charged QDs arrange themselves outside of the micro-nanostructures. This is surprising, if it would be electric mechanisms that were in play, the structures should attract the positively charged QDs instead of repelling them. Indicating that the physical morphology has a greater impact.

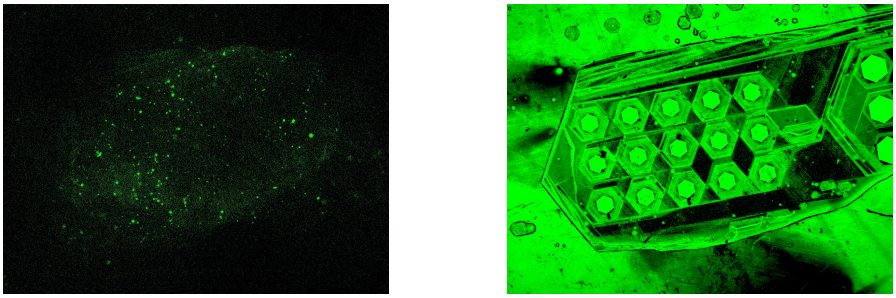

(a) B-2A filter depicting QD's fluorescence

(b) DIA-ILL filter depicting surface topology

Figure 18: Image depicting the droplet after evaporation. Magnification: 2.5x/0.075

Figure 18 depicts the droplet of positively charged QDs on top of the sample. When studying the entire droplet of positively charged QDs on top of the sample, the QDs seem to have distributed themselves randomly. Implying that the evaporation of the

solvent does not affect the distribution of the positively charged QDs as it has affected the negatively charged QDs.

Back of Sample

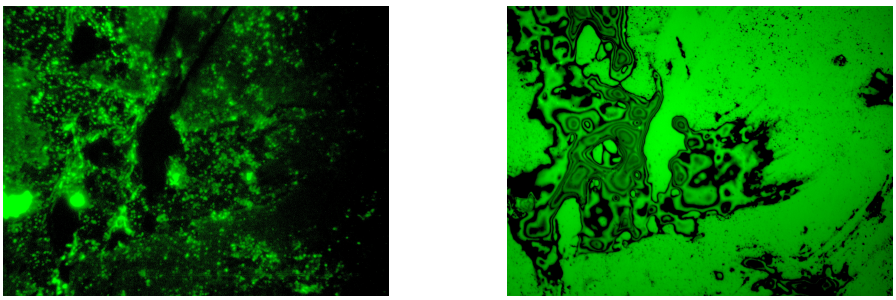

(a) B-2A filter depicting QD's fluorescence

(b) DIA-ILL filter depicting surface topology

Figure 19: Image of QDs on back of the domain. Magnitude: 100x/0.95

Figure 19 depicts the positively charged QDs within the domains on the back of the sample. When the positively charged QDs were studied, no distinct patterns were observed in contrast to the patterns of the negatively charged QDs. This observation was probably due to the lack of physical edging on the surface.

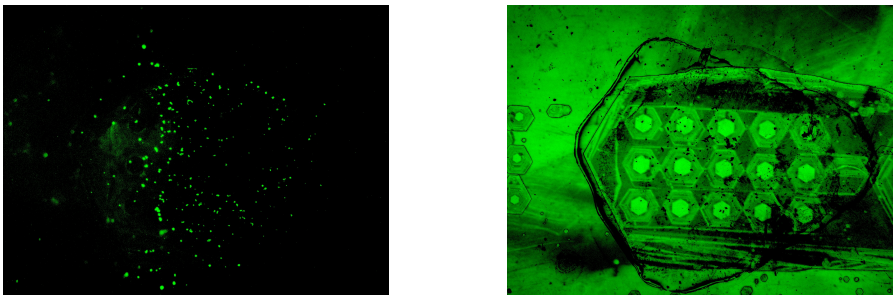

(a) B-2A filter depicting QD's fluorescence

(b) DIA-ILL filter depicting surface topology

Figure 20: Image depicting the droplet after evaporation. Magnification: 2.5x/0.075

Figure 20, depicts the positively charged QDs on the back of the sample after the droplet has evaporated. The QDs seem to be randomly distributed, just as on the top of the sample, indicating that the impact of evaporation does not seem to affect the self-assembly of the positively charged QDs.

4 Discussion

4.1 Analysis of Result

When studying the fluorescence properties of the QDs, the filter B-2A was regarded as giving the best imaging of the QD's fluorescence. Subsequently, this filter was used when studying the QDs distribution on the patterned samples.

Based on the results that were obtained, it is possible to draw several conclusions regarding parameters that affect the distribution of the QDs. Primarily, depending on the solution of QDs, a difference in how the QDs arrange themselves is present. When the images of the evaporated droplets, namely Figures 14, 16, 18 and 20, are compared it is clear that the evaporation of the different solvents have affected the distribution differently. The solvents of the droplets containing the negatively charged QDs, see Figures 14 and 16, seem to have evaporated and driven the QDs to the edge of the droplet, creating a ring-like arrangement. In the case of the positively charged QDs, see Figures 14 and 16, the QDs have clustered together and spread themselves out randomly across the droplet. The characteristics of the different solvents can explain this difference. The negatively charged QDs are solved in isopropanol, which is a volatile solvent, this will therefore result in the Marangoni Effect and create ring patterns. The positively charged particles are instead dispersed in water, which does not seem to have high enough volatility for this effect.

The images portraying the negative QDs seem to confirm that the different sides of the sample has different impacts on the self-assembly. Both images of the entire droplets, see Figures 14a and 16a, depict the Marangoni Effect as well as cracks caused by evaporation, confirming that the evaporation affects the distribution. However, when the magnification increases, differences arise. In Figures 12 and 13 the top of the sample is depicted, and the QDs have self-assembled into dendrite-like structures. However, the patterns are not consistent and do not cover the micro-nano structures. Possible explanations are that the micro-nano structures are not polarised and therefore have a negatively charged surface,

thus repelling the negatively charged QDs, or that the morphology causes the QDs to arrange themselves along the outside of the structures.

The dendrite-like structures are also seen on the back of the sample, see Figure 15, the difference is that the patterns seem to be consistent and the dendrites are shorter. The back lacks physically edged domains, which confirms that the physically edged micro-nano structures impact the arrangement. If the charge of the surface affected the arrangement, it would also be visible on the back. The domains on the back are expected to have a negatively charged surface and if the charges affected the QDs then the negative QDs would be expected to be repelled by the domains. However, this does not seem to be the case. The crystallised structures on the back also seem to have shorter dendrites than those on the top of the sample, which perhaps can be explained by the charges. However, this would need to be studied further in depth.

The arrangement of the positively charged QDs proved to be less consistent than that of the negatively charged QDs. When viewing the evaporated droplets in Figures 18 and 20 there is no distinct pattern, the QDs seem to be scattered randomly. As the magnification increases in Figures 17 and 19, the QDs have not arranged themselves according to a pattern. In all the images of the positive QDs, the fluorescence seems weaker than in the images of the negative QDs, indicating a lower concentration in the solution, thus, explaining why no patterns are seen in higher magnification. Dendrite structures are formed as a result of local inter-particle forces, with a lower concentration these attractions are not as prevalent. As a result there is a lack of crystallised patterns. However, just like in the case of the negatively charged QDs, the QDs on the top of the sample do not distribute themselves within the micro-nano structures, as is seen in Figure 17. If it would be the charges that affected, then the QDs would have arranged themselves within the structures instead, which confirms that the morphology plays a key role. In Figure 19, which portrays the positive QDs on the back of the sample, also indicates that no electric charges seem to affect the QDs as the distribution seems to be random.

In conclusion, generally it does not seem like the charged surfaces of the poled domains

have the strongest impact on the self-assembly. Instead the physical morphology of the sample's structure seems to affect the distribution the most.

4.2 Further Studies

In order to draw further conclusion regarding how a poled sample of $LiNbO_3$ affects the self-assembly of QDs, further studies would have to be executed. It is relevant to study the fluorescence properties of the poled domains of $LiNbO_3$ in order to understand if this affects the images. Furthermore, it is of great interest to change parameters such as temperature, solvent and concentration in order to see how they affect the arrangement of the QDs. If it is better understood how these parameters affect the self-assembly, it would benefit previously mentioned applications such as biological imaging, LED screens and solar cells. It is also worthwhile to attempt to eliminate these parameter's effects in order to understand the electric mechanisms of the poled domains on the QDs better.

5 Acknowledgements

I would like to express my sincere gratitude towards my mentor, Associate Professor Katia Gallo, for all the support as well as constant positivity during this period. I am also very much obliged for the assistance of my lab partner, Yassir Fathullah, who always was present in times when technological expertise was needed as well as for providing me with meaningful discussions regarding the results. Finally I would also like to thank the Rays program, specifically Anna Broms, Isak Nilsson, Serhat Aktay and Klara Kiselman, for guidance, assistance and the opportunity to be a part of this project. Also a special thanks to Rays' collaborators Tekniska museet and Teknikföretagen for enabling this possibility.

References

[1] National Renewable Energy Laboratory. *NREL and Partners Demonstrate Quantum Dots that Assemble Themselves* [Online]. United States of America: U.S. Department of Energy; 2013 [updated 2013 Feb 8; cited 2016 July 2]. Available from: `http://www.nrel.gov/news/press/2013/2113`

[2] Boxberg F, Tulkki J. *Optical Properties of Semiconductor Quantum Dots* [licentiate thesis the Internet]. Netherlands: Gildeprint; 2011 [cited date 2016 July 2]. Available from: `http://www.kth.se/polopoly_fs/1.646894!/perinetti.pdf`

[3] Boxberg F, Tulkki J. *Quantum Dots: Phenomenology, Photonic and Electronic Properties, Modeling and Technology.* [licentiate thesis the Internet]. Netherlands: Gildeprint; 2011 cited date 2016 July 2]. Available from `https://spie.org/samples/PM129.pdf`

[4] Quantum Dots [Online]. Nature; [cited date: July 2 2016]. Available from: `http://www.nature.com/subjects/quantum-dots`

[5] Wüst G, Munsch M, Maier F, Kuhlman A, Ludwig A. D, Wieck A, et. al. *Quantum dots: Artificial atoms for quantum optics.* Nature. 2006;Vol.5: 855 - 856.

[6] Encyclopædia Britannica. *Fluorescence* [Online]. Encyclopædia Britannica, Inc.; 2016[cited date 2016 July 9]. Available from:`http://school.eb.co.uk/levels/advanced/article/472350`

[7] Aldrich Materials Science. *Quantum Dots* [Online]. Sigma-Aldrich; 2016 [cited date: 2016 July 9] Available from: `http://www.sigmaaldrich.com/materials-science/nanomaterials/quantum-dots.html#applications`

[8] Nature Photonics. *The rise of colloidal quantum dots.* [Online]. Macmillan Publishers Limited; 2009 [cited date: 2016 July 9]. Available from: `http://www.nature.com/nphoton/journal/v3/n6/full/nphoton.2009.76.html`

[9] V. Shevchenko E, V. Talapin D. *Self-assembly of semiconductor nanocrystals into ordered superstructures.* Argonne, IL, USA. Chicago, IL, USA: Springer Vienna; 2008: 119-169.

[10] Hammond, P. T. *Surface-Directed Colloid Patterning: Selective Deposition via Electrostatic and Secondary Interactions.* Colloids and Colloid Assemblies. 2004; 317-339

[11] Yang Y, Volmering J, Junkin M, Kin Wong P. *Comparative assembly of colloidal quantum dots on surface templates patterned by plasma lithography.* Soft Matter. 2011;7

[12] Manzo M. *Engineering ferroelectric domains and charge transport by proton exchange in lithium niobate.* [doctoral thesis]. Stockholm, Sweden: KTH Royal Institute of Technology; 2015 [cited date: 10 July 2016]

[13] Lee D. U, Kim D. H, Choi D. H, Kim S. W, Lee H. S, Yoo K, et. al. *Microstructural and optical properties of CdSe/CdS/ZnS core-shell-shell quantum dots*. The Optical Society of America. Vol. 24(2)

[14] Smith A. M, Nie S. *Semiconductor Nanocrystals: Structure, Properties, and Band Gap Engineering*. ACS Publications. 2009;43(2):190–200

[15] Tian J. editor. *Molecular Imaging: Fundamentals and Applications*. China: Springer Science & Business Media; 2013

[16] Ball Z. *Optical Issues in Photolithography*. Rice University. [cited date: 10 July 2016] available from: `http://archive.cnx.org/contents/0661ebbe-52fb-48b1-a96a-0878fa6270ed@4/optical-issues-in-photolithography`

[17] Gaylord T. K, Weis R. S. *Lithium niobate: Summary of physical properties and crystal structure*. Applied Physics A. 1985; Vol.37(4): Årtal;volym(nummer):191-203.

[18] Rice G. *Fluorescent Microscopy* [Online]. Montana State University: Microbial Life Educational Resources; [updated date November 19 2013;cited date July 10 2016]. Available from `http://serc.carleton.edu/microbelife/research$_$methods/microscopy/fluromic.html`

[19] Liljeborg A. *Fluorescence microscope & cooled CCD camera* [Online.] Sweden: KTH Royal Institute of Technology;[cited date: July 10 2016]. Available from: `http://www.nanophys.kth.se/nanophys/facilities/fluormicr/fluormicr.html`